

Biogenic silver nanocomposite TFC nanofiltration membrane with antifouling properties

Shasha Liu¹, Manying Zhang¹, Fang Fang¹, Li Cui¹, Jun Jie Wu², Kaisong Zhang^{1*}

¹Key Laboratory of Urban Pollutant Conversion, Institute of Urban Environment, Chinese Academy of Sciences, Xiamen, 361021, China.

²School of Engineering and Computing Sciences, Durham University, Durham DH1 3LE, UK

* Corresponding author: K. S. Zhang, Tel/ Fax: +86 592 6190782. Email: ks Zhang@iue.ac.cn

Author: Shasha Liu, Tel:+86 592 6190540. Email: ssliu@iue.ac.cn

Author: Manying Zhang, Tel:+86 592 6190540. Email: myzhang@iue.ac.cn

Author: Fang Fang, Tel:+86 592 6190534. Email: ffang@iue.ac.cn

Author: Li Cui, Tel:+86 592 6190534. Email: lcui@iue.ac.cn

Author: Junjie Wu: Tel: +44 191 33 42440 junjie.wu@durham.ac.uk

ABSTRACT

Biofouling is still a major obstacle hindering wider application of thin-film composite (TFC) nanofiltration membranes in the water industry. One of the practical strategies to reduce biofouling is to develop novel anti-biofouling membrane materials. Well-dispersed biogenic silver nanoparticles with a diameter of ~6 nm (Bio-Ag⁰-6) were first immobilized in the selective layer of thin-film composite (TFC) nanofiltration membranes. Different dosages of Bio-Ag⁰-6 were added in the aqueous solution during the interfacial polymerization of tetraethylenepentamine (TEPA) and 1,3,5-benzenetricarbonyl trichloride (TMC). Improved properties of Bio-Ag⁰-6 /TFC membranes were systematically investigated. When the concentration of Bio-Ag⁰-6 increased from 0 wt.% to 0.05 wt.% in aqueous solution, the water flux of TFC membranes increased from 7.31 Lm⁻²h⁻¹ to 13.76 Lm⁻²h⁻¹, while maintaining the rejection of Na₂SO₄ at a relatively high level. The addition of Bio-Ag⁰-6 also enhanced the hydrophilicity of Bio-Ag⁰-6 /TFC membranes in comparison with the

1 bare TFC membranes. All Bio-Ag⁰-6 /TFC membranes exhibited an obvious
2 antibacterial ability to inhibit the growth of *P. aeruginosa*. Moreover, the Bio-Ag⁰-6
3 /TFC membranes showed the property of a low silver leaching rate in both the static
4 immersion and the filtration systems. It demonstrated that the embedded Bio-Ag⁰-6 in
5 TFC membrane via interfacial polymerization improved the performance of the TFC
6 nanofiltration membrane.

7 **Key words:** nanofiltration; biogenic silver nanoparticles; interfacial polymerization,
8 antibacterial; silver leaching rate.

1 **1. Introduction**

2 Membrane fouling is a major obstacle in thin-film composite (TFC) membrane
3 application[1], since fouling causes various negative effects on membrane
4 performance such as decreased permeate flux and increased energy and maintenance
5 costs [2, 3]. In terms of fouling components, fouling can be classified into three types:
6 biofouling, organic fouling, and inorganic fouling [4]. Among them, biofouling is the
7 most complicated, which drastically hinders the application of membrane processes[5].
8 Membrane biofouling is initiated by the adhesion of one of more bacteria to the
9 membrane surface, followed by the growth and multiplication of the sessile cells,
10 which can eventually develop a biofilm on the membrane surface[6]. Unlike physical
11 or chemical fouling, biofouling is difficult to eliminate and causes irreversible damage
12 to the membranes[7]. A common method to mitigate biofouling is feed water
13 pretreatment. Physical pretreatments and chemical pretreatments are able to control
14 scaling, inorganic, and parts of organic fouling. However, most antifouling measures
15 by pretreatments are not effective in eliminating biofouling[8].

16 Recently, the combination of polymeric materials with nanoparticles has
17 attracted much attention in TFC membrane fabrication. The addition of nanoparticles
18 has introduced the concept of thin film nanocomposite (TFN) membranes, which offer
19 enhanced performance of membranes, such as reduced fouling, antimicrobial ability,
20 and other new functionalities[9]. Lee et al. [10] fabricated TFC membranes with TiO₂
21 (~30nm) nanoparticles in the selective layer through interfacial polymerization. Jin et
22 al. [11] prepared polyamide (PA) thin film NF membranes with nano-SiO₂ (~15nm)
23 by interfacial polymerization. The addition of SiO₂ in the PA membrane improved the
24 antifouling ability and increased the pure water flux without significant reduction of
25 salt rejection. Lind et al. [12] prepared Zeolite-polyamide thin film nanocomposite
26 membranes by interfacial polymerization using particles of three sizes (100 nm, 200
27 nm and 300 nm) added in the TMC solution. The result demonstrated that smaller
28 zeolites produced greater enhancement in membrane permeability. These

1 nanoparticles can improve the antifouling ability of the TFC membranes.

2 Due to their excellent antibacterial properties and low toxicity to human cells [3,
3 13, 14], silver nanoparticles (AgNPs) have become an effective addition for fouling
4 mitigation in polymeric membranes. Recently, efforts have been devoted to
5 immobilize AgNPs into the selective layer of a membrane or grafted onto membrane
6 surfaces. Lee et al. [15] added AgNPs in the oil phase to form a polyamine (PA)
7 thin-film layer during the interfacial polymerization. Kim et al. [16] incorporated
8 AgNPs into the MPD aqueous solution during the interfacial polymerization to
9 improve antifouling properties of a TFC membrane. Yin et al. [17] attached AgNPs to
10 the surface of PA TFC membrane effectively via covalent banding, with cysteamine
11 as a bridging agent. These researches indicate that AgNPs can be immobilized to the
12 TFC membrane via different methods and that positioning the AgNPs at the interface
13 of a membrane allows for direct contact of AgNPs with bacterial cells for increased
14 antimicrobial performance.

15 AgNPs in the aforementioned reports (diameter 15~100 nm) are all synthesized
16 via chemical reduction. Chemically produced AgNPs often have problems in particle
17 stability and tend to aggregate at high concentrations or when the average particle size
18 is less than 40 nm. [18]. In addition, most physical and chemical methods are energy
19 intensive or environmentally unfriendly, due to the use of toxic solvents or additives
20 [19]. Hence a more environment-friendly method, the biosynthesis of AgNPs, has
21 been developed. Scientists have already tried to use biological materials for the
22 synthesis of AgNPs. Bacteria, fungi and some plant extracts are capable of producing
23 AgNPs by reducing silver ions [20, 21]. Some researchers have incorporated bio-Ag⁰
24 into different casting solutions to fabricate ultrafiltration (UF) membranes [14, 22].
25 These nanocomposite membranes showed improved antibacterial activity and could
26 be applied to the treatment of drinking water. However, bio-Ag⁰ is not yet known to
27 be used in the fabrication of TFC nanofiltration membranes.

28 In our previous work, novel biogenic silver nanoparticles were reported using

1 dried *Lactobacillus fermentum* biomass [23, 24]. Biogenic silver nanoparticles with an
2 average diameter of ~6 nm (Bio-Ag⁰-6) showed high stability in aqueous solution.
3 The attachment of the nanoparticles with the micro scale surface of the bacterium on
4 which they were formed prevents them from aggregating. The Bio-Ag⁰-6 exhibited
5 excellent antibacterial and anti-biofouling performance in an ultrafiltration membrane.
6 The AgNPs acted via direct interaction of the bacterial cells, the release of silver ions
7 (Ag⁺) and the generation of reactive oxygen species (ROS) [25]. Morones et al. [26]
8 indicated that the bactericidal properties of the nanoparticles were size-dependent, and
9 nanoparticles that present a direct interaction with the bacteria preferentially have a
10 diameter of approximately 1-10 nm. The size of Bio-Ag⁰-6 is very small,

11 In this study, the anti-biofouling characteristics of TFC nanofiltration membrane
12 embedded with Bio-Ag⁰-6 as anti-microble agent were investigated. The effect of
13 different contents Bio-Ag⁰-6 (0.005, 0.025, and 0.05 wt.%) on the permeate flux and
14 anti-biofouling properties was systematically investigated. The SEM, FT-IR, AFM,
15 water contact angle measurements, silver leaching test were also carried out to
16 investigate the membrane surface morphology, its structure and the stability of silver
17 in the membrane. Furthermore, the flux and salt rejection of the Bio-Ag⁰-6 contained
18 TFC membranes after 4 month immersion experiment were tested, to evaluate
19 whether the addition of Bio-Ag⁰-6 in TFC membrane may influence the permeability
20 of TFC membrane after part of the AgNPs release.

21 **2. Experimental**

22 *2.1. Materials*

23 Polysulfone (PS Solvay P3500) was bought from BASF (China) Co. Ltd.
24 Polyvinylpyrrolidone (PVP-K30), triethylamine (TEA; ≥99%), sodium dodecyl
25 sulfate (SDS; 99%), N-hexane (99%), sodium sulfate (Na₂SO₄), ammonia solution
26 (analytical grade), silver standard solution (1000 mg L⁻¹) were supplied by Sinopharm
27 Chemical Reagent Co., Ltd. N,N-dimethylacetamide (DMAc; ≥99%) was sourced
28 from Jinshan Jingwei Chemical Co. Ltd, China. Silver nitrate (AgNO₃, analytical

1 grade) was purchased from Shanghai Shenbo Chemical Co., Ltd.
2 Tetraethylenepentamine (TEPA; 95%), and trimesoyl chloride (TMC; 98%) were
3 purchased from Aladdin Co. Ltd.

4 *2.2. Preparation of PS support membrane*

5 The PS support membrane was prepared via the immersion precipitation phase
6 inversion method. First, the blend solution was prepared by dissolving 18 wt.% PS in
7 DMAc at 80 °C. After stirring for 12h, the homogeneous solution was kept at room
8 temperature to remove air bubbles for around 12h. Then the dope solution was cast
9 onto a non-woven fabric (thickness 100–110 μm) using a casting knife, followed by
10 dipping the membrane into a deionized water bath for immediate phase inversion. The
11 wet film thickness was controlled at ~200 μm. After 30 min in a gelation medium, the
12 membrane was taken out and kept in 1 wt.% NaHSO₃ solution.

13 *2.3. Synthesis and characterization of biogenic silver nanoparticles (Bio-Ag⁰-6)*

14 The biogenic silver nanoparticles (Bio-Ag⁰-6) were synthesized with
15 *Lactobacillus fermentum* LMG 8900 as reported in a previous work [23]. The detailed
16 procedure was as followed: dried biomass was dissolved to in Milli-Q water in an
17 Erlenmeyer flask, with NaOH and diamine silver added sequentially. The final
18 concentration of biomass, silver and [OH]⁻¹ was controlled to 10 g L⁻¹, 10g L⁻¹ and
19 0.2 mol L⁻¹, respectively. After incubating in a shaking incubator at 30°C (200 rpm)
20 for 24h, the solution was centrifuged at 5,000 rpm for 6 min. The biogenic silver
21 hydrosol was separated and centrifuged at 6,000 rpm for 10 min for further
22 concentration and purification. The concentration of biogenic silver nanoparticles is
23 450 mg Ag g⁻¹, which determined by inductively coupled plasma-optical emission
24 spectrometer (ICP-OES).

25 *2.4. Preparation of TFC NF membranes*

26 The TFC NF membrane was prepared by interfacial polymerization of TEPA and
27 TMC as described elsewhere [27, 28]. The aqueous solutions were prepared according
28 to the compositions given in Table 1, and stirred vigorously until completely

1 dissolved. Firstly, the PS support layer was immersed in the aqueous phase for 10 min.
2 The excess solution was removed from the soaked surface by an air knife. Then the
3 organic solution of TMC (0.5 wt.%) in n-hexane was poured over the membrane for
4 20 s to finish the interfacial polymerization reaction. The PS membrane was taken out
5 from the n-hexane solution and heated in an oven at 40°C for about 2 min, for a better
6 polymerization reaction. Finally, the prepared TEPA/TMC composite nanofiltration
7 membranes were rinsed and stored in distilled water.

8 *2.5 Characterization of biogenic silver nanoparticles*

9 To verify the reduction of silver ions, UV-visible analysis was carried out with a
10 UV-vis spectrophotometer (DR5000 HACH) operating in the absorbance mode in the
11 range of 200–600 nm. Distilled water was used as the blank. The size and
12 morphology of the AgNPs were studied by transmission electron microscopy (TEM)
13 (Tecnai F30). Size characterization of the samples was carried out on TEM images
14 using Digital Micrograph software (Gatan Pleasanton, CA, USA). The data were
15 statistically analyzed using SPSS 18.0 software (Armonk, NY, USA).

16 *2.6. Membrane characterization*

17 The surface morphologies of the composite membranes were observed by a field
18 emission scanning electron microscope (FESEM, HITACHI S-4800) at an
19 accelerating voltage of 5 kV. Before SEM analysis, all membrane samples were dried
20 in a vacuum oven at 80°C for more than 48h and coated with gold. Presence of silver
21 nanoparticles was confirmed by energy dispersive X-ray spectra (EDX).

22 The functional groups of membrane surfaces were identified by ATR FT-IR
23 spectroscopy, which was conducted on the Nicolet iS10 (Thermo Fisher Scientific)
24 equipped with multi-reflection Smart Performer ATR accessory. All spectra included
25 the wave numbers from 500 to 4000 cm^{-1} with 64 scans at a resolution of 4.0 cm^{-1} .

26 The root mean square (RMS) roughness of the composite membranes was
27 measured with an Atomic Force Microscope (AFM) MFP-3D (Asylum Research).
28 Air-dried membrane samples were fixed on a specimen holder where $5\mu\text{m} \times 5\mu\text{m}$

1 areas were scanned by a tapping node in the air. Three different images from each
2 membrane sample were analyzed and their average values were taken as the final
3 results.

4 Hydrophilicity of the membrane surface was assessed according to the pure
5 water contact angle, which was measured by the sessile drop method on a video
6 contact angle system (DSA100, German KRUSS). The contact angle was measured
7 automatically by a video camera in the instrument using the drop shape analysis
8 software. At least five measurements on different locations of each sample were
9 performed to calculate an averaged value of contact angles.

10 The filtration performances of the composite membranes were evaluated by a
11 dead-end filtration cell (Model 8010, Millipore Corp. USA). The membranes (4.1cm²
12 of effective area) were operated at 25°C and 0.35 MPa. Pure water flux was measured
13 by the weight of permeate water at a constant transmembrane pressure. The weight of
14 the permeate flux was recorded by a precision electronic balance (Denver Instrument,
15 USA). 2000 ppm Na₂SO₄ was used as feeding solutions to test membrane rejection.
16 The pure water flux and salt rejection was calculated with Eqs. (1) and (2),
17 respectively.

$$18 \quad J = \frac{W_p}{At} \quad (1)$$

$$19 \quad R = \left(1 - \frac{C_p}{C_f}\right) \times 100\%$$

20 (2)

21 Where J is the permeate flux (Lm⁻²h⁻¹), W_p the permeate volume (L), A the
22 membrane area (m²), t the filtration time (h), R the rejection ratio, and C_p and C_f the
23 conductivities of permeate and feed solution, respectively. All the results presented
24 are average data with standard deviation from at least three samples of each type of
25 membrane.

26 2.7. Antibacterial assessment

27 *P. aeruginosa* (ATCC27853) was inoculated into a liquid lysogeny broth (LB)

1 and incubated in an Incubator Shaker (Zhicheng, ZHWY-2012C) shaking at 180 rpm
2 for 10h at 37°C. The resulting cell suspension was further diluted to approximately
3 3×10^6 colony-forming units (CFU)/mL. Aliquots (100 μ l) of the diluted working
4 suspension inoculated with *P. aeruginosa* were applied to agar plates evenly.
5 Membrane samples (diameter 2.1cm) were then placed onto the nutrient agar plates
6 with the selective layer in contact with the agar surface. After incubation at 37°C for
7 24h, the bacterial inhibition zone of each plate was observed. Furthermore, the
8 membrane samples taken from the agar plates were dried in an oven at 80°C for 24h,
9 and coated with platinum using a sputter coater for SEM observation.

10 *2.8. Stability of the immobilized silver*

11 The stability of the immobilized silver on the prepared composite nanofiltration
12 membrane was evaluated via both static release and filtration experiments. In the
13 static release test, the composite nanofiltration membrane was cut into a circular
14 shape with an area of 3.6cm², and was subsequently soaked in a sealed flask filled
15 with 10 ml of Milli-Q water at room temperature. At specified time intervals, the
16 water samples were collected and acidified by 2% HNO₃ to be analyzed by
17 inductively coupled plasma mass spectrometry (ICP-MS, Agilent, model 7500CX).

18 The silver release rate under the filtration condition was evaluated by driving DI
19 water through the membrane at a constant pressure of 0.35MPa. The permeate water
20 was collected every 1.5h and released silver concentration measured by ICP-MS as
21 described above.

22 To measure the silver content incorporated in the composite membrane, the
23 membrane was digested by sonication in concentrated HNO₃ for 3 days. After
24 digestion, the suspension was filtered to remove large particles and analyzed by
25 ICP-MS for total silver content

26 Further, the effect of silver depletion on the change of composite membranes
27 filtration performance was also studied. First, the initial pure water flux and Na₂SO₄
28 rejection of the composite membranes were measured. Then the membranes were

1 immersed in 1% NaHSO₃ for 4 months then 2% HNO₃ for 48h, to maximize the
2 release of silver. After that, the pure water flux and Na₂SO₄ rejection were tested
3 again. Based on the data before and after immersion, the rates of flux and rejection
4 variation can be calculated.

5 **3. Results and Discussion**

6 *3.1. Characterization of Bio-Ag⁰-6.*

7 From the TEM image of Bio-Ag⁰-6 in Fig. 1(a), it was found that biogenic silver
8 nanoparticles were well dispersed and have a spherical morphology. The average
9 diameter was about 6.1 nm calculated by the software image J. The absorption spectra
10 of TEPA aqueous solutions containing different amounts of Bio-Ag⁰-6 were shown in
11 Fig. 1(b). A well-defined peak centered at 420nm was observed, corresponding to the
12 plasmon excitation of AgNPs [15].

13 *3.2. Characterization of the Bio-Ag⁰-6 immobilized TFC membranes*

14 The chemical structure of the selective layer was analyzed by ATR-FTIR
15 spectroscopy, a convenient method to analyze the various chemical bonds in the
16 outermost part of a membrane. The spectra for the PS support membrane and TFC
17 membranes containing different concentrations of Bio-Ag⁰-6 are presented in Fig.2.
18 Besides the typical PS bonds of the substrate, all spectra of TFC membranes M0, M1,
19 M2, M3 exhibited additional absorption peaks at 1637cm⁻¹ and 3378cm⁻¹, which were
20 associated to C=O stretching vibration and N-H stretching vibration bands of amide
21 groups [28]. These characteristic bands proved that the polyamide was formed on the
22 surface of the PS substrate during the interfacial polymerization reaction. Compared
23 to the spectrum of the bare composite NF membrane (M0), those of Bio-Ag⁰-6/TFC
24 membranes (M1, M2, M3) were weaker. This may be attributed to two reasons: (i) the
25 Bio-Ag⁰-6 which covered on the surface of the composite membranes decreased the
26 signals of the absorption peaks. (ii) the extent of interfacial polymerization reaction
27 was relatively reduced with the addition of Bio-Ag⁰-6.

28 Images of TFC membranes containing different concentrations of Bio-Ag⁰-6 are

1 shown in Fig. 3(a). With the increase Bio-Ag⁰-6 concentration in the aqueous phase,
2 the colour of the composite membrane varied from white to tints of yellow, indicating
3 that the immobilized amount of Bio-Ag⁰-6 in the selective layer increased. Fig. 3(b)
4 shows the surface morphologies of TFC membranes with different concentrations of
5 Bio-Ag⁰-6 added in the aqueous solution during the interfacial polymerization
6 reaction. All of these membranes exhibited typical “ridge and valley” structure
7 characteristic of the PA thin-film layer of TFC membrane[29]. Compare to the NF
8 membrane without Bio-Ag⁰-6 (M0), the membrane with 0.005% Bio-Ag⁰-6 in
9 aqueous solution (M1) has a relatively looser nodular structure. It is probably
10 attributed to that the addition of hydrophilic Bio-Ag⁰-6 enhanced the tension between
11 the aqueous phase and oil phase and reduced the mass transfer of TEPA to organic
12 phase. When the concentration of Bio-Ag⁰-6 in aqueous solution increased to 0.05%,
13 the ultra-thin layer surface became looser, which resulted in the increase of membrane
14 permeability and decrease of the salt rejection. The EDS spectra results (Table 2)
15 indicated that the Bio-Ag⁰-6 had successfully immobilized in the selective layer of the
16 Bio-Ag⁰-6/TFC membranes (M1, M2, M3). As the Bio-Ag⁰-6 content increased in the
17 aqueous solution, the EDS spectra of Ag became stronger, especially for M3. Both the
18 photos of the membranes and the EDS spectra proved that the content of AgNPs
19 increased with the increased concentration of Bio-Ag⁰-6 in aqueous solution during
20 interface polymerization.

21 Fig. 4 presents AFM images of composite membranes (M0 and M1). A summary
22 of the surface roughness values of the composite membranes are listed in Table 2.
23 Root-mean-square (RMS) height is a key physical parameter determined by AFM
24 analysis; it is defined as the mean of the root for deviation from the standard surface
25 to the indicated surface. High RMS means high surface roughness [30]. As shown in
26 Fig.4, the surfaces of the prepared TFC membranes (M0, M1) exhibited abundant
27 nodular structures, a well-known property of conventional interfacial polymerization
28 for polyamide thin-film layers. The RMS of the composite NF membrane was

1 reduced from 25.7 nm for the bare NF membrane (M0) to 10.9 nm for the
2 Bio-Ag⁰-6/TFC membrane (M1). This finding is consistent with the other results
3 where the surface roughness experienced a decrease after the addition of AgNPs [13].
4 In general, all Bio-Ag⁰-6/TFC membranes (M1, M2, M3) had a smoother surface
5 compared with the bare TFC membrane (M0). It is well established that the
6 membrane with lower roughness and surface energy has stronger antifouling abilities
7 [31, 32].

8 Contact angles of TFC membranes (M0, M1, M2, M3) were summarized in
9 Table 2. The contact angle is a measure of tendency for water to wet the membrane
10 surface. A lower contact angle means a better hydrophilicity of the membrane surface.
11 **It has been generally acknowledged that increasing membrane surface hydrophilicity**
12 **could effectively reduce membrane fouling[33].** The contact angle gradually
13 decreased from 41.8° to 33.0° when the Bio-Ag⁰-6 concentration in the aqueous
14 phase increased from 0wt% to 0.05wt%. The addition of Bio-Ag⁰-6 had a great
15 contribution to the surface hydrophilicity. This may attribute to the well dispersed
16 Bio-Ag⁰-6 nanoparticles which contain a great deal of hydrophilic groups such as
17 hydroxyl groups and amino groups, responsible for the hydrophilicity increase.

18 The main chemical components in the selective layer affecting the hydrophilicity
19 of the membrane are amide groups, amino end groups (from the hydrolysis of
20 unreacted acyl chloride groups), and AgNPs. The improved surface hydrophilicity of
21 the TFC membrane prepared from a polymerization reaction of TEPA and TMC is
22 mainly from the increased Bio-Ag⁰-6 content at the surface skin layer.

23 *3.3. Permeate flux and selectivity*

24 The pure water permeability of the TFC membrane with different Bio-Ag⁰-6
25 contents was determined by measuring the pure water flux through a dead-end
26 filtration system. As presented in Table 3, with the increase of Bio-Ag⁰-6 in aqueous
27 solution, the pure water flux of the TFC membranes increased from 7.31 L/m²h to
28 13.76 L/m²h at 0.35 MPa. The presence of Bio-Ag⁰-6 in the aqueous solution during

1 the interfacial polymerization reaction can effectively enhance the water permeability
2 compared with the bare TFC membrane. The pure water flux of the Bio-Ag⁰-6/TFC
3 membrane with AgNPs was higher than that of the bare TFC membrane.

4 The rejection rate of the TFC membrane to salt is mainly determined by both
5 the size and Donnan exclusion effects [34]. In Table 3, when the concentrations of
6 Bio-Ag⁰-6 increased from 0wt% to 0.025wt% in the aqueous solution, the salt
7 rejection of the prepared Bio-Ag⁰-6/TFC membranes slightly decreased from 88.46%
8 to 86.71%. When the concentration of Bio-Ag⁰-6 reached 0.05wt%, the rejection
9 decreased drastically to 68.33%. This may be due to the high concentration of
10 Bio-Ag⁰-6 in aqueous phase blocking the degree of TEPA/TMC chemical
11 cross-linking, resulting in a loose membrane structure, which will increase pore size
12 and weaken the size exclusion effect. The results were consistent with the SEM
13 images.

14 3.4. Anti-bacterial tests

15 *P. aeruginosa* was chosen as the test bacteria in the disk diffusion test. The
16 results shown in Fig. 5 indicated that the prepared Bio-Ag⁰-6/TFC membranes had a
17 significant inhibition capacity to the *P. aeruginosa*. The bare TFC membrane did not
18 show any inhibition effect toward the growth of *P. aeruginosa*. With the increase of
19 Bio-Ag⁰-6 content, the inhibition zone became clearer and larger. Although there was
20 no obvious inhibition zone around membrane M1, the amount of *P. aeruginosa*
21 attached to the surface of the membrane decreased evidently. Both of M2 and M3 had
22 a clear bacterial inhibition zone.

23 Fig. 6 shows the SEM images of bacteria grown on different types of membranes
24 taken from the disk diffusion experiment. It can be observed that the surface of the
25 bare TFC membrane (M0) was covered with a dense layer of bacteria. The results for
26 the Bio-Ag⁰-6/TFC membranes were quite different from that of bare TFC membrane.
27 Less bacteria was observed on the membrane surface and the membranes with higher
28 silver loading (M2 and M3) seemed nearly free of bacterial growth. The results may

1 be attributed to the higher hydrophilicity, the lower roughness and the bactericidal
2 effects of AgNPs [35, 36].

3 Some researches explained that the anti-bacterial capacity of silver composite
4 membranes mainly relies on their ability to release silver ions (Ag^+), which has a
5 strong toxicity to bacteria. Silver ions can react with cysteine by replacing the
6 hydrogen atom of the thiol group to form S-Ag complexes [37], thus might altering
7 protein structure and hindering enzyme action, particularly respiratory function.
8 Furthermore, Ag^+ can influence the structure and the permeability of the cell
9 membrane [38, 39].

10 The above results clearly indicate that the incorporation of Bio-Ag⁰-6 can
11 effectively enhance the antibacterial performance of the TFC membranes.

12 *3.5. Analysis of silver leaching*

13 The release rate of silver from the selective layer of the TFC membrane was
14 examined in both static and filtration experiments. As presented in Fig. 7, the initial
15 silver ions released from M1, M2, M3 were 0.013, 0.16 and 0.20 $\mu\text{g cm}^{-2} \text{day}^{-1}$,
16 respectively, which then declined steadily with time. The release rate of M1, M2, M3
17 leveled off to a level below 0.01 $\mu\text{g cm}^{-2} \text{day}^{-1}$ after being soaked in Milli-Q water for
18 40 days, The total amount of Bio-Ag⁰-6 immobilized in the selective layer of TFC
19 membranes M1, M2, M3 were 1.05, 3.61 and 4.96 $\mu\text{g cm}^{-2}$, respectively. After 40
20 days of the static release test, the ratio of the remaining silver to the original amount
21 in the Bio-Ag⁰-6/TFC membranes were 97%, 89% and 75% for M1, M2 and M3,
22 respectively. Due to the relatively low leaching rate of around 0.01 $\mu\text{g cm}^{-2} \text{day}^{-1}$, all
23 the membranes are expected to last more than 5 months until all the silver in the
24 membranes is completely released. This will potentially extend the life of the
25 antifouling effect of the TFC membrane.

26 The concentration of silver ions in the permeate fluid during filtration was
27 analyzed by ICP-MS. The result is presented in Fig. 8. For all the tested membranes,
28 Ag^+ leaching increased at a higher Bio-Ag⁰-6 content. The leaching Ag^+ concentration

1 in the permeate side was very low with an initial concentration being less than 25 ppb
2 for M3, and less than 5 ppb for M1 and M2. The release rate of Ag^+ gradually
3 decreased as more water was filtered with time. According to the National Secondary
4 Drinking Water Regulations, the Ag threshold is limited to 100 ppb. Hence, the
5 amount of silver released from the prepared Bio- Ag^0 -6/TFC membranes (M1, M2 and
6 M3), has no health concern. According to the filtration experiment, the prepared TFC
7 membranes with Bio- Ag^0 -6 could be a good choice for membrane biofouling
8 disinfection since the Ag^+ release was below the threshold value during the filtration
9 process. The leaching results suggested that the antimicrobial effect of Bio- Ag^0 -6
10 could last for a long time.

11 Although the anti-bacterial action by AgNPs is not fully studied, several
12 researchers inferred that the anti-bacterial capacity of the composite membranes is
13 based on their ability to release biotoxic silver ions (Ag^+) into the surrounding
14 solution [40]. Several studies have proved that the anti-bacterial capacity of silver
15 loaded membranes had a significant reduction due to a decrease of the silver content
16 [41]. In this study, after 40 days soaking process, most of the silver remained inside
17 the membranes.

18 As shown in Fig. 9, the Bio- Ag^0 -6/TFC membranes (M1 and M2) show an
19 excellent stability of flux and selectivity. After the membranes soaked in NaHSO_3 for
20 4 month and in 2% HNO_3 for 48 h, the Na_2SO_4 rejection of bare TFC membrane (M0)
21 is 74.08%, only 88% compared with the initial rejection of M0. that Na_2SO_4 rejections
22 of Bio- Ag^0 -6/TFC (M1, M2) were 80.63% and 83.25%, respectively. The rejections
23 of M1 and M2 were more than 91% compared with the initial rejection of M1 and M2.
24 The result indicated that the Bio- Ag^0 -6 nanoparticles may have a strong binding
25 strength with the PA polymer and could be held tightly in the selective layer which is
26 consistent with the results of the silver leaching during the 12 h filtration. The release
27 of silver from the membrane may form the outer surface of the selective layer of the
28 TFC membrane. So it is expected that a kind of stable and novel anti-biofouling TFC

1 nanofiltration membrane could be achieved.

2 **4. Conclusions**

3 The improved properties of the TFC nanofiltration membranes were achieved by
4 adding Bio-Ag⁰-6 in aqueous solution during interfacial polymerization. The
5 following conclusions can be drawn from the experimental results.

6 (1) The Bio-Ag⁰-6 was successfully introduced in the selective layer of the TFC
7 membranes. Bio-Ag⁰-6 enhanced the hydrophilicity and decreased the
8 surface roughness value of the TFC membranes, which may reduce the
9 attachment of microbes.

10 (2) The addition of Bio-Ag⁰-6 can improve the permeability of the TFC
11 membrane. Both membranes M1 and M2 showed higher pure water flux
12 compared to the bare TFC membrane (M0), while maintaining a high
13 rejection to Na₂SO₄.

14 (3) In terms of bacterial analysis, the Bio-Ag⁰-6/TFC membranes exhibited
15 excellent anti-biofouling performance. The results demonstrated that the
16 Bio-Ag⁰-6 nanoparticles in the TFC membranes could be an effective
17 approach to reduce membrane biofouling.

18 (4) The released silver from the Bio-Ag⁰-6/TFC membranes were in the safe
19 range and had less influence on the filtration performance compared to the
20 bare TFC membrane, indicating the stability of immobilized silver in the
21 membranes.

22 **Acknowledgements**

23 KSZ thanks Royal Academy of Engineering, UK for the Research Exchange
24 with China/India scheme. The authors gratefully acknowledge the financial support of
25 Xiamen Municipal Bureau of Science and Technology (3502Z20131159). The authors
26 are also grateful to Dr Steve Chapman from The James Hutton Institute for polishing
27

1 manuscript and insightful comments.

2 **References**

- 3 [1] E. Bar-Zeev, I. Berman-Frank, B. Liberman, E. Rahav, U. Passow, T. Berman,
4 Transparent exopolymer particles: Potential agents for organic fouling and biofilm
5 formation in desalination and water treatment plants, *Desal.Wat. Treat.*, 3 (2009)
6 136-142.
- 7 [2] H. Wu, B. Tang, P. Wu, Preparation and characterization of anti-fouling
8 β -cyclodextrin/polyester thin film nanofiltration composite membrane,
9 *J.Membr.Sci.*, 428 (2013) 301-308.
- 10 [3] A. Dror-Ehre, A. Adin, H. Mamane, Control of membrane biofouling by silver
11 nanoparticles using *Pseudomonas aeruginosa* as a model bacterium, *Desal.Wat.*
12 *Treat.*, 48 (2012) 130-137.
- 13 [4] S. Kappachery, D. Paul, J. Yoon, J.H. Kweon, Vanillin, a potential agent to
14 prevent biofouling of reverse osmosis membrane, *Biofouling*, 26 (2010) 667-672.
- 15 [5] H.-L. Yang, J.C.-T. Lin, C. Huang, Application of nanosilver surface modification
16 to RO membrane and spacer for mitigating biofouling in seawater desalination,
17 *Water Res.*, 43 (2009) 3777-3786.
- 18 [6] N. Hilal, V. Kochkodan, L. Al-Khatib, T. Levadna, Surface modified polymeric
19 membranes to reduce (bio) fouling: a microbiological study using *E. coli*,
20 *Desalination*, 167 (2004) 293-300.
- 21 [7] C.X. Liu, D.R. Zhang, Y. He, X.S. Zhao, R. Bai, Modification of membrane
22 surface for anti-biofouling performance: Effect of anti-adhesion and anti-bacteria
23 approaches, *J.Membr.Sci.*, 346 (2010) 121-130.
- 24 [8] T. Kim, Y. Kim, Y. Choi, J. Kweon, J. Song, N. Gang, Biofilm formation and its
25 effect on biofouling in RO membrane processes for wastewater reuse, *Desal.Wat.*
26 *Treat.*, 2 (2009) 71-75.
- 27 [9] M.M. Pendergast, E.M.V. Hoek, A review of water treatment membrane
28 nanotechnologies, *Energ. Environ. Sci.*, 4 (2011) 1946.
- 29 [10] H.S. Lee, S.J. Im, J.H. Kim, H.J. Kim, J.P. Kim, B.R. Min, Polyamide thin-film
30 nanofiltration membranes containing TiO₂ nanoparticles, *Desalination*, 219 (2008)
31 48-56.
- 32 [11] L. Jin, W. Shi, S. Yu, X. Yi, N. Sun, C. Ma, Y. Liu, Preparation and
33 characterization of a novel PA-SiO₂ nanofiltration membrane for raw water
34 treatment, *Desalination*, 298 (2012) 34-41.
- 35 [12] M.L. Lind, A.K. Ghosh, A. Jawor, X. Huang, W. Hou, Y. Yang, E.M. Hoek,
36 Influence of zeolite crystal size on zeolite-polyamide thin film nanocomposite
37 membranes, *Langmuir*, 25(2009) 10139-10145.
- 38 [13] J. Huang, H.T. Wang, K.S. Zhang. Modification of PES membrane with Ag-SiO₂:
39 reduction of biofouling and improvement of filtration performance. *Desalination.*,
40 2014. 336:8-17.

- 1 [14] M. Zhang, K. Zhang, B. De Gusseme, W. Verstraete, Biogenic silver
2 nanoparticles (bio-Ag₀) decrease biofouling of bio-Ag₀/PES nanocomposite
3 membranes, *Water Res.*, 46 (2012) 2077-2087.
- 4 [15] S.Y. Lee, H.J. Kim, R. Patel, S.J. Im, J.H. Kim, B.R. Min, Silver nanoparticles
5 immobilized on thin film composite polyamide membrane: characterization,
6 nanofiltration, antifouling properties, *Polym. Adv. Technol.*, 18 (2007) 562-568.
- 7 [16] E.-S. Kim, G. Hwang, M. Gamal El-Din, Y. Liu, Development of nanosilver and
8 multi-walled carbon nanotubes thin-film nanocomposite membrane for enhanced
9 water treatment, *J.Membr.Sci.*, 394-395 (2012) 37-48.
- 10 [17] J. Yin, Y. Yang, Z. Hu, B. Deng, Attachment of silver nanoparticles (AgNPs)
11 onto thin-film composite (TFC) membranes through covalent bonding to reduce
12 membrane biofouling, *J.Membr.Sci.*, 441 (2013) 73-82.
- 13 [18] F. Mafuné, J.-y. Kohno, Y. Takeda, T. Kondow, H. Sawabe, Structure and
14 stability of silver nanoparticles in aqueous solution produced by laser ablation,
15 *J.Phys.Chem.B*, 104 (2000) 8333-8337.
- 16 [19] J. Huang, G. Arthanareeswaran, K. Zhang, Effect of silver loaded sodium
17 zirconium phosphate (nanoAgZ) nanoparticles incorporation on PES membrane
18 performance, *Desalination*, 285 (2012) 100-107.
- 19 [20] R.S. Patil, M.R. Kokate, S.S. Kolekar, Bioinspired synthesis of highly stabilized
20 silver nanoparticles using *Ocimum tenuiflorum* leaf extract and their antibacterial
21 activity, *Spectrochim. Acta A*, 91 (2012) 234-238.
- 22 [21] V.K. Sharma, R.A. Yngard, Y. Lin, Silver nanoparticles: green synthesis and
23 their antimicrobial activities, *Adv. Colloid Interfac.*, 145 (2009) 83-96.
- 24 [22] B. De Gusseme, T. Hennebel, E. Christiaens, H. Saveyn, K. Verbeken, J.P. Fitts,
25 N. Boon, W. Verstraete, Virus disinfection in water by biogenic silver
26 immobilized in polyvinylidene fluoride membranes, *Water Res.*, 45 (2011)
27 1856-1864.
- 28 [23] M. Zhang, K. Zhang, B. De Gusseme, W. Verstraete, R. Field, The antibacterial
29 and anti-biofouling performance of biogenic silver nanoparticles by *Lactobacillus*
30 *fermentum*, *Biofouling*, 30 (2014) 347-357.
- 31 [24] M. Zhang, R. Field, K. Zhang, Biogenic silver nanocomposite polyethersulfone
32 UF membranes with antifouling properties, *J.Membr.Sci.*, (2014).
- 33 [25] Q. Bao, D. Zhang, P. Qi, Synthesis and characterization of silver nanoparticle
34 and graphene oxide nanosheet composites as a bactericidal agent for water
35 disinfection, *J. Colloid Interface Sci.*, 360 (2011) 463-470.
- 36 [26] J.R. Morones, J.L. Elechiguerra, A. Camacho, K. Holt, J.B. Kouri, J.T. Ramirez,
37 M.J. Yacaman, The bactericidal effect of silver nanoparticles, *Nanotechnology*, 16
38 (2005) 2346-2353.
- 39 [27] X. Fan, Y. Dong, Y. Su, X. Zhao, Y. Li, J. Liu, Z. Jiang, Improved performance
40 of composite nanofiltration membranes by adding calcium chloride in aqueous
41 phase during interfacial polymerization process, *J.Membr.Sci.*, 452 (2014) 90-96.
- 42 [28] Y. Li, Y. Su, Y. Dong, X. Zhao, Z. Jiang, R. Zhang, J. Zhao, Separation

- 1 performance of thin-film composite nanofiltration membrane through interfacial
2 polymerization using different amine monomers, *Desalination*, 333 (2014) 59-65.
- 3 [29] J. Xiang, Z. Xie, M. Hoang, D. Ng, K. Zhang, Effect of ammonium salts on the
4 properties of poly(piperazineamide) thin film composite nanofiltration membrane,
5 *J.Membr.Sci.*, 465 (2014) 34-40.
- 6 [30] L. Li, S. Zhang, X. Zhang, Preparation and characterization of
7 poly(piperazineamide) composite nanofiltration membrane by interfacial
8 polymerization of 3,3',5,5'-biphenyl tetraacyl chloride and piperazine,
9 *J.Membr.Sci.*, 335 (2009) 133-139.
- 10 [31] A. Razmjou, J. Mansouri, V. Chen, The effects of mechanical and chemical
11 modification of TiO₂ nanoparticles on the surface chemistry, structure and fouling
12 performance of PES ultrafiltration membranes, *J.Membr.Sci.*, 378 (2011) 73-84.
- 13 [32] Y. Chen, Y. Zhang, H. Zhang, J. Liu, C. Song, Biofouling control of halloysite
14 nanotubes-decorated polyethersulfone ultrafiltration membrane modified with
15 chitosan-silver nanoparticles, *Chem. Eng. J.*, 228 (2013) 12-20.
- 16 [33] H. Yu, Y. Zhang, J. Zhang, H. Zhang, J. Liu, Preparation and antibacterial
17 property of SiO₂-Ag/PES hybrid ultrafiltration membranes, *Desal.Wat. Treat.*, 51
18 (2013) 3584-3590.
- 19 [34] S. Yu, Q. Zhou, S. Shuai, G. Yao, M. Ma, C. Gao, Thin-film composite
20 nanofiltration membranes with improved acid stability prepared from
21 naphthalene-1,3,6-trisulfonylchloride (NTSC) and trimesoyl chloride (TMC),
22 *Desalination*, 315 (2013) 164-172.
- 23 [35] Y. Xiong, Y. Liu, Biological control of microbial attachment: a promising
24 alternative for mitigating membrane biofouling, *Appl.Microbiol.Biot.*, 86 (2010)
25 825-837.
- 26 [36] P. Landini, D. Antoniani, J.G. Burgess, R. Nijland, Molecular mechanisms of
27 compounds affecting bacterial biofilm formation and dispersal,
28 *Appl.Microbiol.Biot.*, 86 (2010) 813-823.
- 29 [37] H. Basri, A. Ismail, M. Aziz, Polyethersulfone (PES)-silver composite UF
30 membrane: effect of silver loading and PVP molecular weight on membrane
31 morphology and antibacterial activity, *Desalination*, 273 (2011) 72-80.
- 32 [38] L. Cui, P. Chen, S. Chen, Z. Yuan, C. Yu, B. Ren, K. Zhang, In situ study of the
33 antibacterial activity and mechanism of action of silver nanoparticles by
34 surface-enhanced Raman spectroscopy, *Anal. Chem.*, 85 (2013) 5436-5443.
- 35 [39] Q. Feng, J. Wu, G. Chen, F. Cui, T. Kim, J. Kim, A mechanistic study of the
36 antibacterial effect of silver ions on *Escherichia coli* and *Staphylococcus aureus*,
37 *J.Biomed.Mater.Res.*, 52 (2000) 662-668.
- 38 [40] X. Cao, M. Tang, F. Liu, Y. Nie, C. Zhao, Immobilization of silver nanoparticles
39 onto sulfonated polyethersulfone membranes as antibacterial materials,
40 *Colloid.Surface.B*, 81 (2010) 555-562.
- 41 [41] W.L. Chou, D.G. Yu, M.C. Yang, The preparation and characterization of
42 silver - loading cellulose acetate hollow fiber membrane for water treatment,

- 1 Polym. Adv. Technol., 16 (2005) 600-607.
- 2
- 3
- 4

1 Table 1

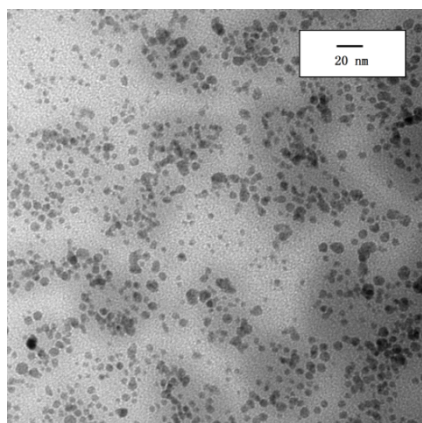
2 Composition of the aqueous solution with different bio-Ag⁰-6

NO.	TEPA(wt%)	TEA(wt%)	SDS(wt%)	Bio-Ag ⁰ -6(wt%)
M0	1	1	0.12	0
M1	1	1	0.12	0.005
M2	1	1	0.12	0.025
M3	1	1	0.12	0.05

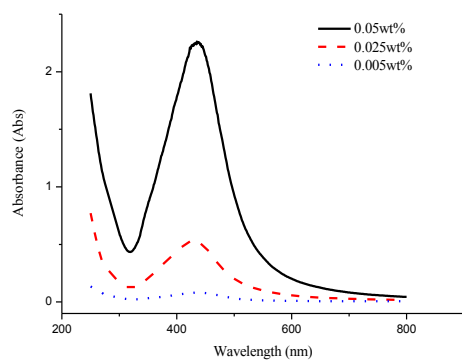
3

4

1 (a)



(b)

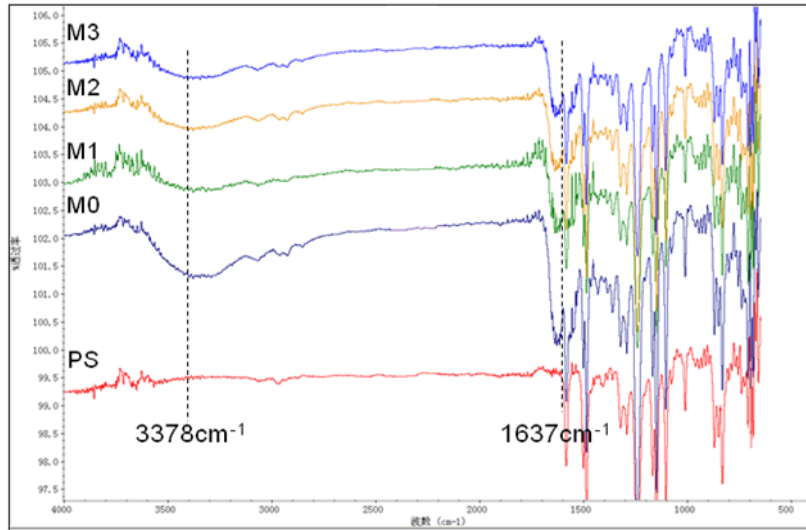


2

3

4

Fig.1 TEM image of Bio-Ag⁰-6(a) and UV-vis absorption spectra of Bio-Ag⁰-6 suspension (b).



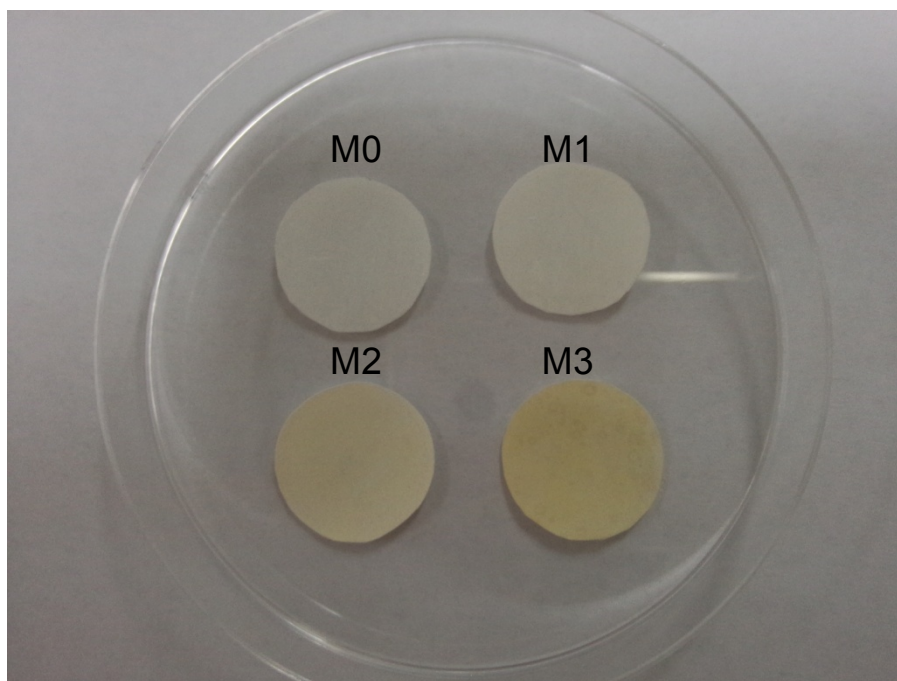
1

2

Fig.2 FT-IR of PS substrate membrane and TFC membrane M0, M1, M2, M3.

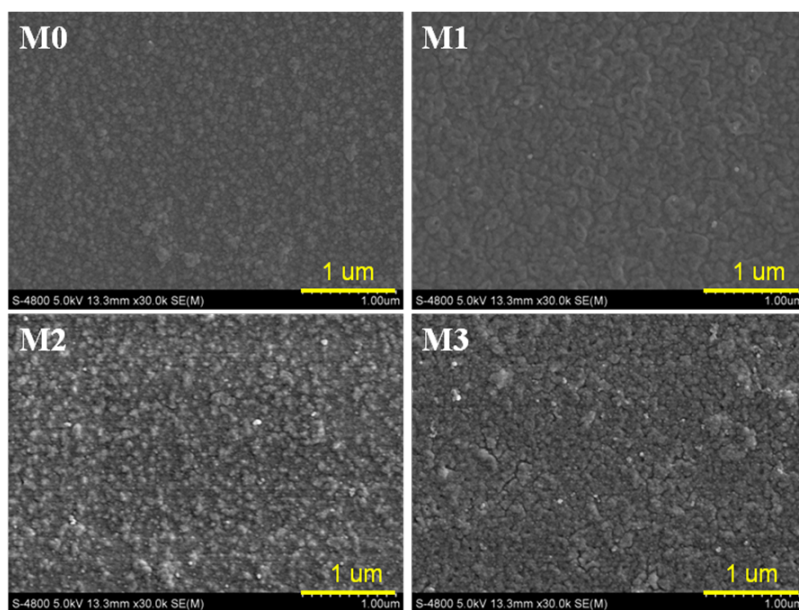
3

1 (a)



2

3 (b)



4

5 Fig.3 (a) images of TFC membrane samples, (b) SEM images of M0, M1, M2, M3.

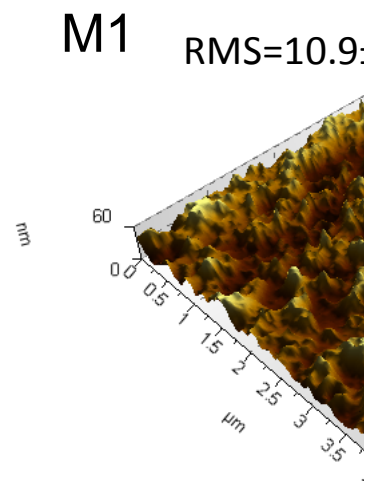
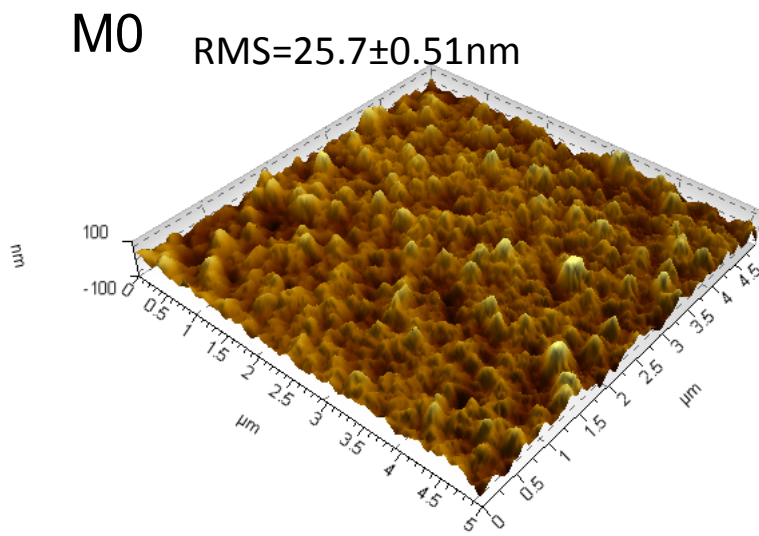
6

1 Table 2.

2 Surface elemental composition of M0, M1, M2, M3

Membrane samples	Element				
	Ag (%)	C (%)	O (%)	S (%)	Au (%)
M0	0	3.18	1.14	8.82	86.86
M1	0.25	2.72	0.63	7.64	88.76
M2	1.63	2.62	0.78	7.67	87.30
M3	2.71	2.17	1.08	7.27	86.24

3



- 1
- 2 Fig.4 AFM images of bare TFC membrane (M0) and nano-composite TFC membrane (M1).
- 3

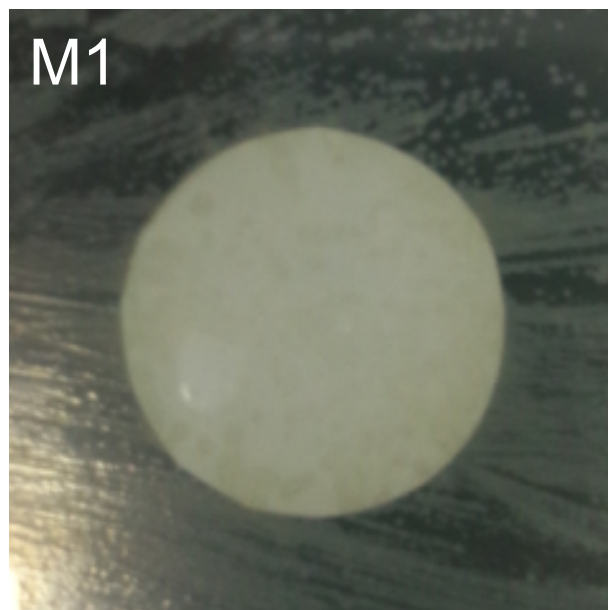
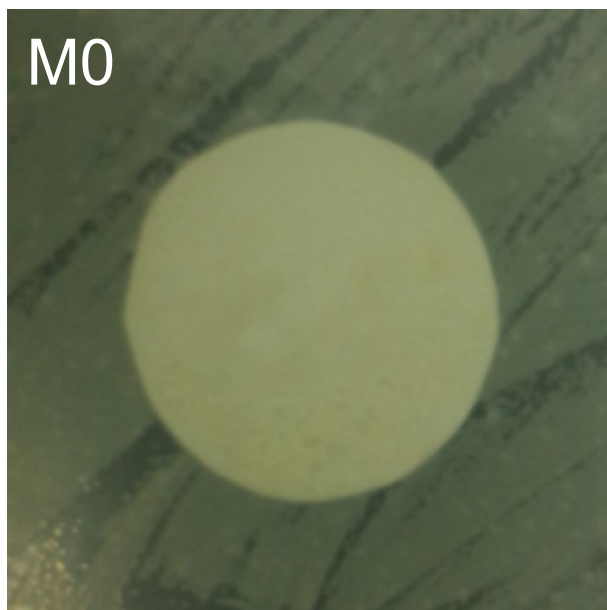
1 Table 3

2 Roughness, contact angle, pure water flux and salt rejection of the prepared TFC membranes

Membrane	Roughness (nm)	Contact angle (°)	Water flux (L/m ² h)	Rejection of Na ₂ SO ₄ (%)
M0	25.7±0.51	41.8±0.94	7.31±2.7	88.46±2.2
M1	10.9±0.82	38.6±1.28	9.88±0.5	87.95±2.2
M2	8.05±4.31	37.8±0.94	10.34±0.1	86.71±2.5
M3	20.3±0.57	33.0±0.91	13.76±3.0	68.33±1.3

3 (2000 ppm Na₂SO₄, 0.35 MPa)

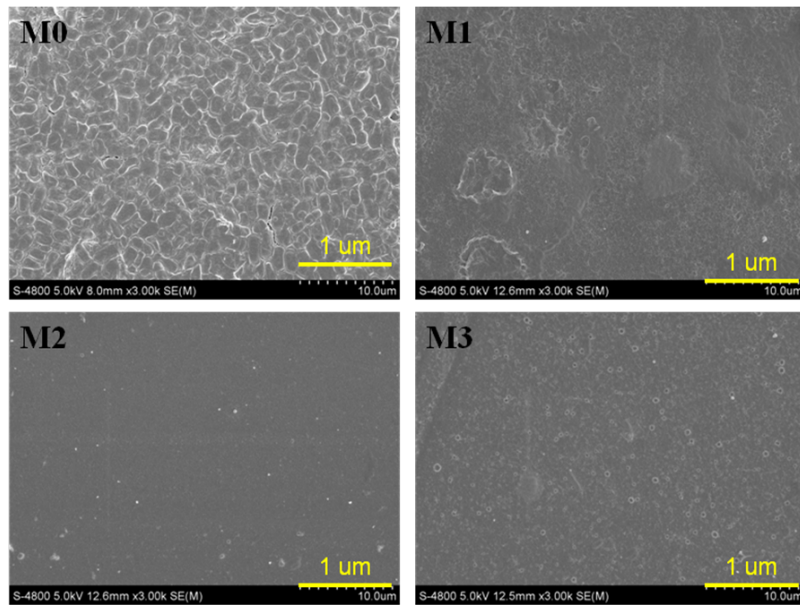
4



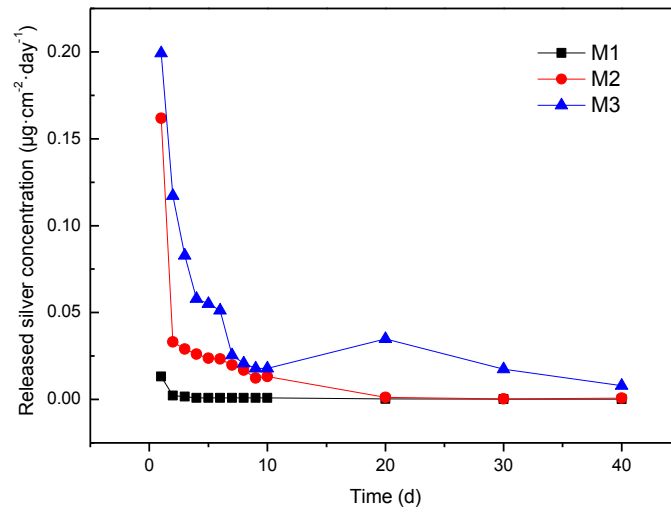
1

2

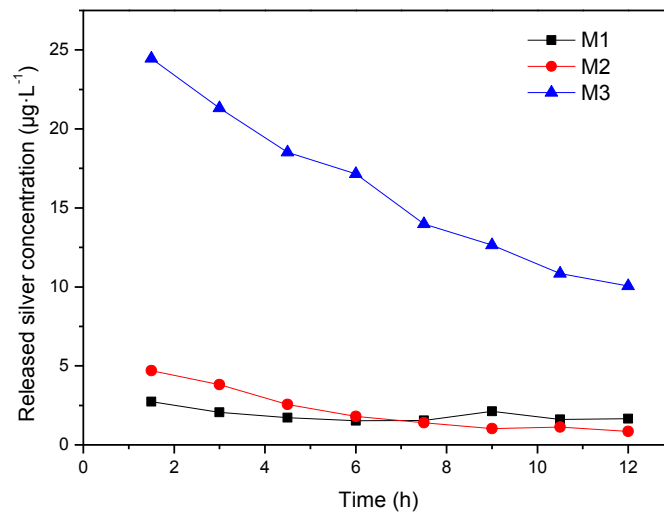
Fig.5 Inhibition zone for *P.aeruginosa* (PA) on composite NF membranes M0, M1, M2, M3.



1
2 Fig.6 SEM images of TFC membranes M0, M1, M2, M3 after batch incubation with *P.*
3 *aeruginosa* (PA) at 37°C for 24h.
4



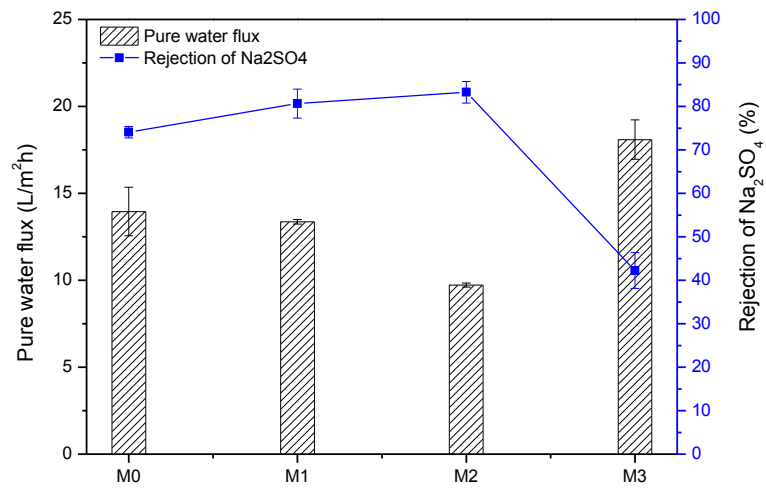
1
2 Fig. 7 The release rate of silver during 40 days leaching test.
3



1

2 Fig. 8 Concentration of leached silver in the solutions filtered by the test membranes M1, M2, M3.

3



1
 2 Fig.9 The pure water flux and salt rejection of M0, M1, M2, M3 after silver depletion
 3 treatment (soaked in 1% NaHSO₃ for 4 month and 2% HNO₃ for 48 h).
 4